The 15th International Symposium on Magnetic Bearings, August 3-6, 2016, Mojiko Hotel, Kitakyushu, Japan

ISMB15

Control of Magnetic Bearings with Rotor-Mounted MEMS Accelerometers

Samuel JIMÉNEZ* and Patrick KEOGH*

* Department of Mechanical Engineering, University of Bath

Claverton Down, Bath, BA2 3JB, United Kingdom

E-mail: s.jimenez@bath.ac.uk

Abstract

Mounting MEMS accelerometers inside hollow shaft rotors has been proposed as a novel sensor design for vibration monitoring and control in rotating machinery. The application of this technology to Active Magnetic Bearings (AMB) could allow sensor/actuator collocation. This paper explores the possibility of using rotor-mounted accelerometers as standalone sensors for AMB control. The integration of the acceleration signals, after conversion from the rotating to the inertial reference frame, is considered as a means to extract rotor displacement information. The sensitivity of this method to uncertainty in the measurement of the gravitational component and in the estimation of the initial angular position is studied. The latter produces a steady state error in the rotor position estimation which cannot be measured by the accelerometers. Therefore, a current injection technique has been developed to eliminate this error. The method produces a low-amplitude, high-frequency response in the rotor, which has negligible effect on the rotordynamics, but is easily detected by accelerometers and allows the steady state error to be estimated and reduced. The simulation of a disc being levitated in an AMB system using only internal accelerometers has been undertaken and results are reported.

Key words : Magnetic bearings, Accelerometer, Rotor-mounted sensor, Measurement uncertainty, Control

1. Introduction

Sensing of vibration in rotor systems is typically achieved through the use of fixed eddy current displacement probes. Example applications are Active Magnetic Bearings (AMBs), which rely on such transducers to control the magnetic gap between the rotor and stator. However, Pfister *et al.* (2010) noted that eddy current sensors are dependent on the material and geometry of the rotor, are susceptible to electromagnetic interferences, and are sensitive to the dielectric properties of any gap fluid, which can vary during operation. In AMB systems, having eddy current probes mounted on the stator also leads to issues of non-collocation of sensors and actuators, as these cannot occupy the same physical space. The detrimental effect of such non-collocation has been reported widely (Maslen and Schweitzer, 2009).

A rotor vibration sensing system based on MEMS accelerometers mounted within hollow rotors has been introduced by Jiménez *et al.* (2016). The compact sensing module contains MEMS accelerometers, a microcontroller, and a wireless radio. The design enables an “active rotor”, capable of measuring its own vibration state and transmitting data to an external computer for analysis and control. The potential of such a sensing system lies in its application to AMBs, schematically depicted in Fig. 1. This may allow some of the drawbacks of conventional systems to be overcome.

Accelerometers eliminate the dependence of the sensing on the materials and geometry of the rotor, and on the dielectric properties of the gap fluid. By placing the sensors within the shaft, they can be located at the same axial position as the magnetic bearings to avoid non-collocation. In addition, they are naturally shielded from the working environment. The reduced size of the sensors also enables large numbers of them to be placed along the rotor, improving observability of rotor vibration in general, and allowing sensing at locations with critical components such as seals or turbine blades.

The use of MEMS accelerometers as rotor-mounted sensors has only recently received the attention of the research community. Elnady *et al.* (2013) presented a study in which the output of an accelerometer located on a rotating shaft was modeled. Baghli *et al.* (2010) applied these sensors to measure the instantaneous torque, while Arebi *et al.* (2011) used them to detect misaligned rotor shafts. More particularly, Cole *et al.* (2014) considered the use of internal accelerometers together with stator-mounted eddy current transducers in a sensor fusion scheme for feedback control in AMBs. The

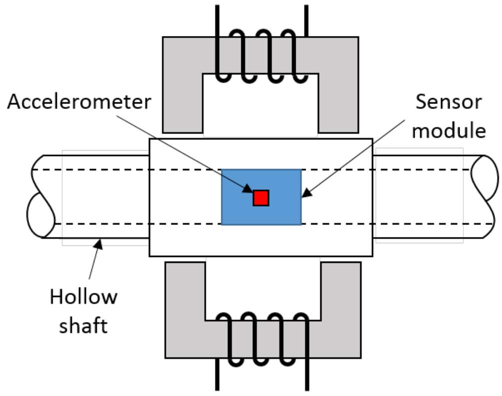

Fig. 1 Schematic of an active magnetic bearing system with internal accelerometers.

approach could provide enhanced control in the face of poor quality position measurements or significant non-collocation of sensors and bearings.

The fundamental aim of this research is to understand whether or not rotor-mounted accelerometers can be used as standalone sensors for control of AMB systems. In this preliminary work, the stable levitation of an unbalanced disc with an on-board accelerometer is explored. The rotor displacement information is derived by integration of the accelerometer signal. As the sensor is located in a rotating frame of reference, transformation to an inertial frame is required. However, errors may be present in the estimation of the gravitational acceleration component and the initial angular position of the rotor. An analysis of their effect on the estimation of the rotor position is undertaken, and methods for mitigating them are introduced. Simulated results of a disc mass levitated on an AMB are presented.

2. Problem formulation

The system under study consists of an unbalanced two-dimensional disc mass suspended on a single eight-pole AMB, depicted in Fig. 2. The disc has mass M, eccentricity e, unbalance phase φ and has a wireless bi-axial MEMS accelerometer located at its geometric centre O. The magnetic gap is h, and the clearance between the disc and an touchdown bearing is c. The displacement of the disc is given by complex parameter $d_r = x + \mathrm{j}y$. The sensor can measure acceleration in the U and V planes of the rotating reference frame. It is assumed that the bearing forces in the X and Y inertial axes are decoupled, so that $F = F_x + \mathrm{j}F_y$, and also depend on the bias and control currents, $i_b = i_{bx} + \mathrm{j}i_{by}$ and $i_c = i_{cx} + \mathrm{j}i_{cy}$, respectively.

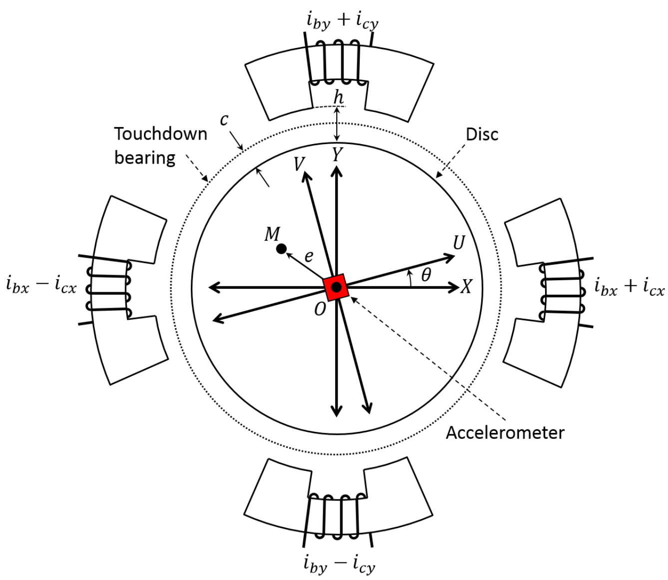

Fig. 2 Schematic of an active magnetic bearing system with internal accelerometers.

To levitate such a disc, a conventional PID controller can be used if the disc displacement information can be extracted from the accelerometer signals. The analytical expression of the output of an accelerometer located inside a rotating shaft has been derived by the authors in (Jiménez *et al.*, 2016) and is given by:

$$a_a(t) = \left(\ddot{d}_r(t) + \mathrm{j}g_a\right)\mathrm{e}^{-\mathrm{j}\theta(t)} \tag{1}$$

where a_a is the accelerometer signal, g_a is the gravitational acceleration and θ is the angle between the inertial XY and rotating UV frames. The rotational speed ω is assumed to be constant and known, and hence $\theta(t) = \omega t + \theta(0)$. Extracting the displacement information requires transforming the signal from the rotating to the inertial reference frame, and then integrating twice. However, uncertainty in g_a and $\theta(0)$ will introduce errors in this process, which must be accounted for.

The sensitivity of accelerometers depends on a number of external factors, such as power supply and ambient temperature. It also varies between devices, due to variability in manufacture. When the accelerometer is rotating at low speeds, this varying sensitivity has a more significant impact on the gravitational component, as it can dominate the accelerometer signal. The term g_a is therefore assumed to be unknown, but constant under steady operating conditions. The initial angular position of the disc with respect to the inertial frame, $\theta(0)$, can be approximated by using the gravitational component when the disc is at zero speed, as $a_a(t) = \mathrm{j}g_a\mathrm{e}^{-\mathrm{j}\theta(t)(0)}$ if $\ddot{d}_r = 0$ in Eq. (1). However, the uncertainty in the gravitational component means the initial angle $\theta(0)$ is also unknown.

As the conversion process requires the unknown g_a and $\theta(0)$, it is necessary to use estimated values g_e and $\theta_e(0)$ instead, and accept the introduction of a certain amount of error. The difference between the real and estimated parameters will be error values, defined as

$$g_\varepsilon = g_a - g_e \tag{2}$$

$$\theta_\varepsilon(0) = \theta(0) - \theta_e(0) \tag{3}$$

Thus, in order to achieve stable levitation using only the disc-mounted accelerometers, it will be necessary to understand and mitigate the effect of error terms g_ε and $\theta_\varepsilon(0)$.

3. Conversion from rotating acceleration to inertial displacement with uncertainty

The conversion process first requires transforming the signal to the inertial frame and subtracting the gravitational acceleration. These operations are carried out using the estimated parameters, so that the accelerometer-based disc acceleration $\ddot{d}_a$ is

$$\ddot{d}_a = a_a\mathrm{e}^{\mathrm{j}\theta_e} - \mathrm{j}g_e = \ddot{d}_r\mathrm{e}^{-\mathrm{j}\theta_\varepsilon(0)} + \mathrm{j}\left(g_a\mathrm{e}^{-\mathrm{j}\theta_\varepsilon(0)} - g_e\right) \tag{4}$$

The second term in Eq. (4) is related to the estimation errors and will grow rapidly if integrated, leading to an erroneous position measurement. However, the term is independent of the motion of the disc, and hence, $\ddot{d}_a(0) = \mathrm{j}\left(g\mathrm{e}^{-\mathrm{j}\theta_\varepsilon(0)} - g_e\right)$ can be obtained from converting the accelerometer signals of a stationary disc, for which $\ddot{d}_r = 0$ in Eq. (4). The signal is then integrated twice to obtain the accelerometer-derived disc velocity $\dot{d}_a$ and displacement d_a, considering the initial condition $\ddot{d}_a(0)$:

$$\dot{d}_a = \int\left(\ddot{d}_a - \ddot{d}_a(0)\right)\,\mathrm{d}t = \dot{d}_r\mathrm{e}^{-\mathrm{j}\theta_\varepsilon(0)} \tag{5}$$

$$d_a = \iint\left(\ddot{d}_a - \ddot{d}_a(0)\right)\,\mathrm{d}t = d_r\mathrm{e}^{-\mathrm{j}\theta_\varepsilon(0)} \tag{6}$$

The true position of the disc within the bearings, p_r, will take into account the initial velocity and position conditions, so that $p_r = d_r + \dot{d}_r(0)t + d_r(0)$. Although these parameters cannot be measured with the accelerometer alone, they can be known under certain conditions. For instance, integration can begin with the disc resting on the touchdown bearing with zero rotational speed, and hence $\dot{d}_r(0) = 0$ and $d_r(0) = -\mathrm{j}c$, where c is the radial clearance. Thus, the accelerometer-derived disc position p_a is given by:

$$p_a = d_r\mathrm{e}^{-\mathrm{j}\theta_\varepsilon(0)} - \mathrm{j}c \tag{7}$$

It follows that

$$p_r = p_a\mathrm{e}^{\mathrm{j}\theta_\varepsilon(0)} + \mathrm{j}c\left(\mathrm{e}^{\mathrm{j}\theta_\varepsilon(0)} - 1\right) \tag{8}$$

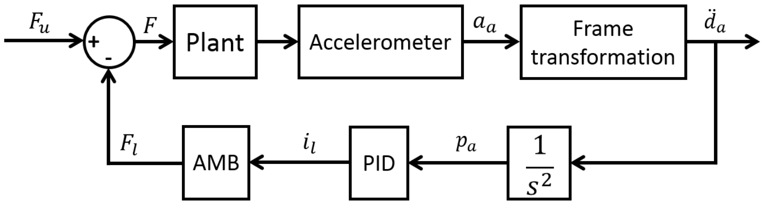

Fig. 3 Block diagram of AMB control system using accelerometer-derived rotor position information.

Hence, the true disc position will be given by p_a, but subject to a phase error and a steady state error. Conventional PID control can be applied to the derived position to achieve stable levitation, so that the system can be represented by the block diagram in Fig. 3

As the control will aim to minimise p_a, the effect of the phase error for small $\theta_\varepsilon(0)$ does not have a significant effect on the disc position. The second term in Eq. (8), however, can be significant, as it constitutes a steady-state position error which depends on the size of the radial clearance c. As the position error cannot be measured by the accelerometer directly, a high-frequency current injection technique has been developed to minimise it.

3.1. High-frequency injection to minimise steady-state error

The technique relies on the position dependence of the AMB force output. If a harmonic force is applied with the AMB, the amplitude of the disc response will be proportional to its position within the bearings. The phase of the response will indicate whether the position is positive or negative. Hence, a low-amplitude, high-frequency harmonic current is injected once p_a is minimised with the control. The resulting force output produces a disc response with small displacement but, crucially, large acceleration, which is easily detected by the accelerometer but has negligible effect on the disc dynamics. The force output when current $i_q = i_{qx} + \mathrm{j}i_{qy}$ is injected is given by

$$F = k_b\left[\left(\frac{(i_{bx}+i_{cx}+i_{qx})^2}{(h-x)^2} - \frac{(i_{bx}-i_x+i_{qx})^2}{(h+x)^2}\right) + \mathrm{j}\left(\frac{(i_{by}+i_y+i_{qy})^2}{(h-y)^2} - \frac{(i_{by}-i_y+i_{qy})^2}{(h+y)^2}\right)\right] \tag{9}$$

where k_b is a bearing constant $k_b = \mu_o N^2 A_h/4$, with μ_o being the permeability of free space, N the number of coils in the magnetic winding, and A_h is the area of the magnetic gap. The control currents satisfy $|i_x| < i_b$ and $|i_y| < i_b$. Considering also the unbalance force F_u, the equation of motion for the disc will be

$$M\ddot{p}_r = F_u + F_c + F_q \tag{10}$$

where $F_c = F_{cx} + \mathrm{j}F_{cy}$ and $F_q = F_{qx} + \mathrm{j}F_{qy}$ are the forces associated with stable levitation and the current injection, respectively. The injected current will be of the form $i_q = Q(1+\mathrm{j})\sin\omega_q t$, with $Q \ll |i_c| < i_b$ and frequency $\omega_q \gg \omega$. Hence,

$$F_{qx} = 2k_b\left(\frac{2Q((h^2+x^2)i_{lx} + 2i_b xh)\sin(\omega_q t) + xhQ^2\left(1-\cos(2\omega_q t)\right)}{(h^2-x^2)^2}\right) \tag{11}$$

$$F_{qy} = 2k_b\left(\frac{2Q((h^2+y^2)i_{ly} + 2i_b yh)\sin(\omega_q t) + yhQ^2\left(1-\cos(2\omega_q t)\right)}{(h^2-y^2)^2}\right) \tag{12}$$

The last terms in Eqs. (11) and (12) are of particular relevance because they are proportional to the disc positions in each axis, x and y, and independent of the control and bias currents. In addition, the distinct frequency component at $2\omega_q$ enables the associated disc response to be isolated using a bandpass filter. Hence, considering only the highest frequency forcing term, the equation of motion for a disc is

$$M\ddot{p}_q = B\cos(2\omega_q t) \tag{13}$$

where p_q is the bandpass-filtered displacement. The amplitude term B is given by

$$B = -2k_b hQ^2\left(\frac{x}{(h^2-x^2)^2} + \mathrm{j}\frac{y}{(h^2-y^2)^2}\right)\cos(2\omega_q t) \tag{14}$$

The amplitude can be linearised around the desired operating point, $x = y = 0$. In this case,

$$B = -\frac{2k_b Q^2}{h^3} p_r \tag{15}$$

For simplicity, it can be assumed that the overall disc motion with and without the injected current is approximately the same and so the contribution of p_q in p_r is negligible, making these variables independent. It follows from classical theory for a forced harmonic oscillator that

$$p_q = P_q \cos(2\omega_q t) \tag{16}$$

$$\ddot{p}_q = -4\omega_q^2 P_q \cos(2\omega_q t) \tag{17}$$

where

$$P_q = \frac{k_b Q^2}{2h^3 \omega_q^2 M} p_r = H p_r \tag{18}$$

Equation (16) shows that the amplitude of the displacement p_q will be small for small Q. However, the presence of the ω_q^2 term in $\ddot{p}_q$ ensures that the acceleration is large for high-frequency injections and, hence, easily detectable by the accelerometers. The disc response $\ddot{p}_q$ can be derived from the accelerometer-inferred disc acceleration signal $\ddot{d}_a$ (Eq. (4)), having accounted for the initial condition $\ddot{d}_a(0)$, by applying a bandpass filter, to yield

$$BP\left(\ddot{d}_a - \ddot{d}_a(0)\right) = \ddot{p}_q \mathrm{e}^{-\mathrm{j}\theta_\varepsilon(0)} \tag{19}$$

A Fast Fourier Transform (FFT) can then be used to obtain the response amplitude and phase of the filtered signal, defined as

$$D_f = \left|BP\left(\ddot{d}_a - \ddot{d}_a(0)\right)\right| = 4\omega^2 H |p_r| \tag{20}$$

$$\phi_f = \arg\left[BP\left(\ddot{d}_a - \ddot{d}_a(0)\right)\right] = \arg p_r - \theta_\varepsilon(0) + \pi \tag{21}$$

Combining Eqs. (8), (20) and (21) yields

$$D_f \mathrm{e}^{\mathrm{j}(\phi_f)} \frac{-1}{4\omega_q^2 H} = p_r \mathrm{e}^{-\mathrm{j}\theta_\varepsilon(0)} = p_a + \mathrm{j}c\left(1 - \mathrm{e}^{-\mathrm{j}\theta_\varepsilon(0)}\right) \tag{22}$$

Therefore, as $p_a \to 0$, being minimised through the control action, $D_f \mathrm{e}^{\mathrm{j}(\phi_f)} / \left(4\omega_q^2 H\right) \to \mathrm{j}c\left(1 - \mathrm{e}^{-\mathrm{j}\theta_\varepsilon(0)}\right)$. This is the change in p_a required to minimise $p_r \mathrm{e}^{-\mathrm{j}\theta_\varepsilon(0)}$, and so the disturbance p_δ can be added to the accelerometer-derived position, where

$$p_\delta = \frac{K_p}{4\omega_q^2 H} \int D_f \mathrm{e}^{\mathrm{j}(\phi_f)} \,\mathrm{d}t \tag{23}$$

and the parameter K_p dictates the response time of the integral action. The new system block diagram is given in Fig. 4.

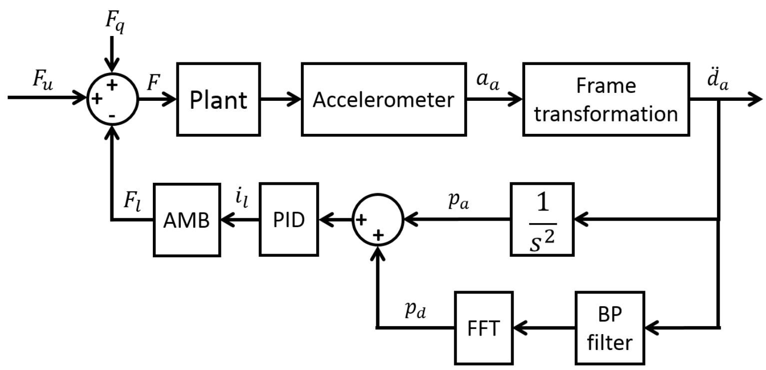

Fig. 4 Block diagram of AMB control system using accelerometer-derived rotor position information together with high-frequency current injection for steady state error correction.

The control will now act on both the estimated disc position and disturbance term together, $p_a + p_\delta$, to minimise $p_r \mathrm{e}^{-\mathrm{j}\theta_\varepsilon(0)}$. Thus the steady state error appearing in Eq. (7) can be reduced and the true disc position will be controlled, despite no direct measurement of it being available. Once $p_a + p_\delta$ has been minimised, $p_a = \mathrm{j}c\left(\mathrm{e}^{-\mathrm{j}\theta_\varepsilon(0)} - 1\right)$, from which the initial angle error can be obtained as

$$\theta_\varepsilon(0) = \mathrm{j}\ln\left(1 - \mathrm{j}\frac{p_a}{c}\right) \tag{24}$$

4. Simulated levitation

The levitation of the disc using the control scheme in Fig. 4 was tested in simulation. The model parameters are given in Table 1. The simulation assumes the disc begins resting on the touchdown bearing with zero rotational speed, and so a controlled levitation from $-jc$ to the centre of the bearings over 5 s is first performed. PID control is applied throughout, using the accelerometer-derived position p_a. The discrepancy between p_a and the true rotor position p_r is clearly observed in Figs. 5 and 6, which show the position of the disc in the Y and X axes, respectively. Despite the fact that the motion of the rotor should take place only in the vertical Y direction, the error manifests itself most prominently in the X axis position, with an error equivalent to approximately 17% of the clearance. In order to minimise this steady state error, a high frequency current is injected into the bearings at 7.5 s. This has a negligible effect on the rotor position, but can be clearly identified in the accelerometer signal, presented in Fig. 7. The correction signal p_d is added to the accelerometer-derived position after 10 s, and so the position error is eliminated. At 20 s the injected current is removed and between 25 and 35 s the rotor speed is ramped up from 0 to 1000 rev/min. The use of the high-frequency current injection allows the steady state error to be minimised while maintaining stable levitation, using only the disc-mounted accelerometers.

Table 1 Simulation parameters

Parameter	Symbol	Value	Units
Disc mass	M	2	Kg
Disc eccentricity	e	1	mm
Unbalance phase	φ	80	deg
Air gap	h	1	mm
Touchdown bearing clearance	c	0.5	mm
Bearing constant	k_b	6.28×10^{-7}	Nm^2/A^2
Bias currents	i_{bx},i_{by}	3	A
PID gain - Proportional	K_P	3.6×10^4	-
PID gain - Derivative	K_D	5.4×10^2	-
PID gain - Integral	K_I	2.2×10^5	-
Initial angular position	$\theta(0)$	150	deg
Initial angular position error	$\theta_\varepsilon(0)$	10	deg
Measured gravity component	g_a	9.5	m/s^2
Estimated gravity component	g_e	9.81	m/s^2
Injected current amplitude	Q	0.1	A
Injected current frequency	ω_q	500	Hz

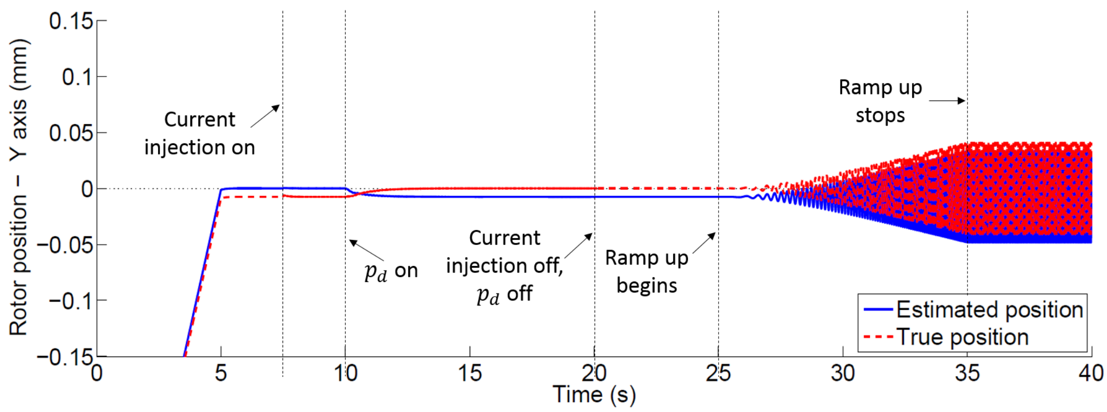

Fig. 5 Y axis rotor position during simulation of stable levitation.

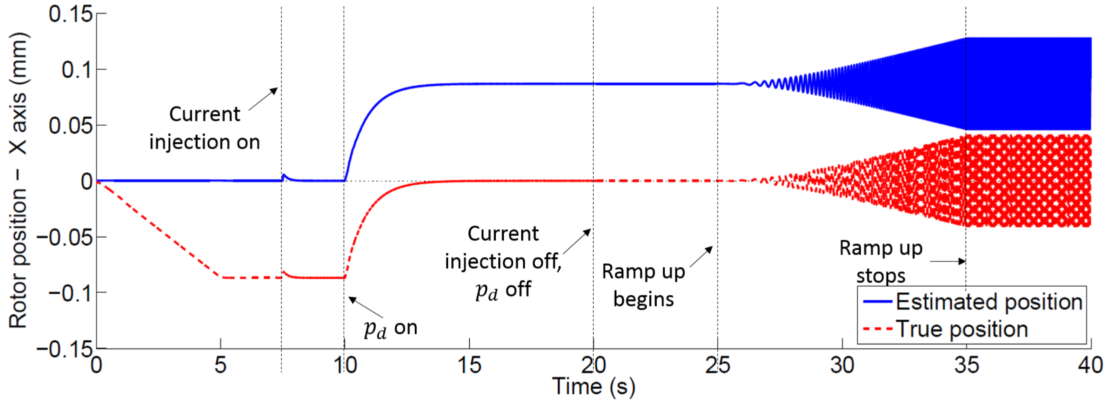

Fig. 6 X axis rotor position during simulation of stable levitation.

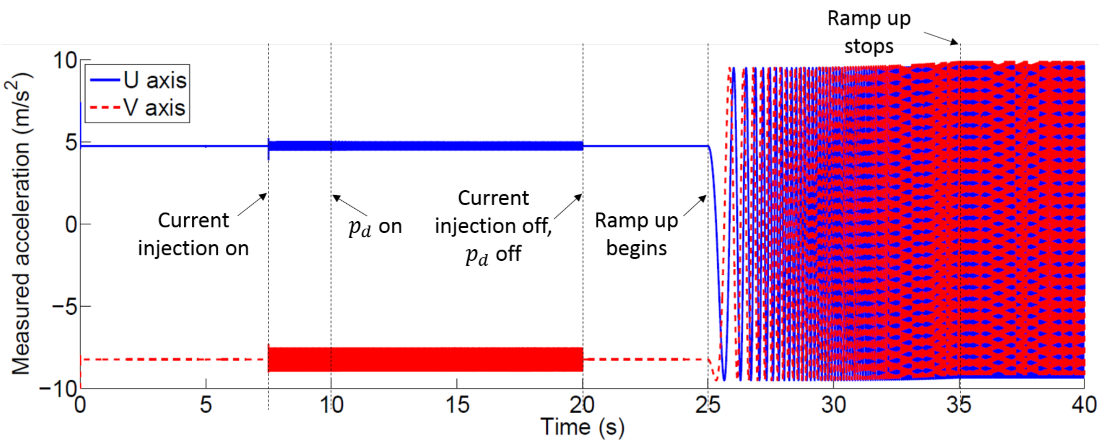

Fig. 7 Accelerometer output during simulated stable levitation.

5. Further work

In this preliminary study, consideration has been given to two sources of error which are unique to sensing with rotor-mounted accelerometer. However, there exist other sources of error which can have a significant effect on the levitation stability, namely sensor saturation, resolution and electrical noise. The former may be overcome by controlling the levitation process so as to ensure that the disc levitates slowly, limiting the maximum acceleration it will be subject to. The latter two, however, present the problem of introducing errors into Eq. (1), so that

$$a_a(t) = \left(\ddot{d}_r(t) + \mathrm{j}g_a\right)\mathrm{e}^{-\mathrm{j}\theta(t)} + f_r(a_a) + f_n(t) \tag{25}$$

where f_r represents a discontinuous function associated with rounding the accelerometer signals to its resolution limit and f_n is a noise function. Even for sensors with good resolution and noise characteristics, the double integration of these error sources can lead to exponential errors in the position estimation. A solution may be to reset the integration under controlled circumstances. To this end, a reference position measurement obtained from an ancillary sensor may be required. Eddy current sensors could be used for rotors which are sufficiently rigid in the operating speed range, even if located far from the AMB. The fusion of both rotor-mounted accelerometers and self-sensing AMB technology emerges as an enticing option, as both sensors can be implemented together at the same plane location. Rotor-mounted accelerometers may prove to be useful as a compliment to other sensing techniques. For instance, the high-frequency current injection technique could be used to produce a reference measurement to prevent the ambiguous signal output associated with magnetic saturation in sensorless bearings (Maslen and Schweitzer, 2009).

6. Conclusions

This paper explores the use of rotor-mounted accelerometers within AMB systems. The principal advantage of these sensors relating specifically to AMBs are avoiding non-collocation of sensors and bearings. In addition they eliminate the system's dependence on the material and geometric properties of the rotor, and on the dielectric properties of the gap fluid.

A possible technique for using rotor-mounted accelerometers as a standalone sensor is estimating the rotor position by double integration of the sensor signal. This process requires transforming the sensor output between the rotating and inertial reference frames. A disc-model has been used to understand the effect of two particular error sources on such a process, namely the gravitational component error and the initial angular position error. The latter produces a steady-state position error which cannot be measured by simple integration alone. Thus, a current injection technique has been introduced which involves generating a low-amplitude, high-frequency response in the rotor, which can be measured by the accelerometers while having a negligible impact on the rotor position. As the response will be position-dependent and the injected frequency is a known parameter, appropriate signal processing can be used to estimate the steady-state position error and minimise it.

The proposed sensing system has been simulated, and results demonstrating the effect of the aforementioned errors have been presented. The simulation shows how a disc can be stably levitated with minimum steady-state position error in an AMB by using on-board accelerometer signals alone. Further work aims to explore the effects of other error sources, such as resolution limits and noise, and consider fusion of different sensors to overcome some of the challenges associated with them. In future, the research will seek to demonstrate whether the levitation can be achieved experimentally.

7. Acknowledgment

The authors would like to extend their gratitude to the Engineering and Physical Sciences Research Council (EPSRC) of the United Kingdom, for supporting the PhD study of Samuel Jiménez through studentship 1223129.

References

Arebi, L., Gu, F., Hu, N. and Ball, A., Misalignment detection using a wireless sensor mounted on a rotating shaft. In *Proceedings of the 24th International Congress on Condition Monitoring and Diagnostics Engineering Management (COMADEM)*, pages 1289–1299, 2011.

Baghli, L., Pautex, J. F. and Mezani, S., Wireless instantaneous torque measurement, application to induction motors. In *19th International Conference on Electrical Machines, ICEM*, Rome Italy, 2010.

Cole, M. O. T., Jiménez, S. and Keogh, P. S., Feedback control of a magnetic bearing using fusion of rotor acceleration and position measurements. In *14th International Symposium on Magnetic Bearings*, Linz, Austria, 2014.

Elnady, M., Abdelbary, A., Sinha, J. and Oyadiji, S., FE and experimental modeling of on-shaft vibration measurement. In *15th International Conference on Aerospace Sciences & Aviation Technology*, pages 1–18, Cairo, Egypt, 2013.

Jiménez, S., Cole, M. O. T. and Keogh, P. S., Vibration sensing in smart machine rotors using internal MEMS accelerometers. *Journal of Sound and Vibration*, 2016, doi: 10.1016/j.jsv.2016.05.014.

Maslen, E. H. and Schweitzer, G., *Magnetic Bearings: Theory, Design, and Application to Rotating Machinery*. Springer, 2009.

Pfister, T., Gunther, P., Dreier, F. and Czarske, J., Dynamic rotor deformation and vibration monitoring using a non-incremental laser doppler distance sensor. In *AIP Conference Proceedings*, volume 1253, page 361, Ancona, Italy, 2010.